Mitochonic acid-5 ameliorates chlorhexidine gluconate-induced peritoneal fibrosis in mice

Hiro Inoue[1], Kenta Torigoe[1], Miki Torigoe[1], Kumiko Muta[1], Yoko Obata[1], Takehiro Suzuki[2], Chitose Suzuki[2], Takaaki Abe[2], Takehiko Koji[3], Hiroshi Mukae[4], Tomoya Nishino[1]

[1]Department of Nephrology, Nagasaki University Graduate School of Biomedical Sciences, Nagasaki, Japan

[2]Division of Nephrology, Endocrinology and Vascular Medicine, Tohoku University Graduate School of Medicine, Sendai, Japan

[3]Department of Histology and Cell Biology, Nagasaki University Graduate School of Biomedical Sciences, Nagasaki, Japan

[4]Department of Respiratory Medicine, Nagasaki University Graduate School of Biomedical Sciences, Nagasaki, Japan

Corresponding author: Kenta Torigoe, MD, PhD

Department of Nephrology, Nagasaki University Hospital, 1-7-1 Sakamoto,

19 Nagasaki 852-8501, Japan

20 Tel: +81-95-819-7282; Fax: +81-95-849-7285

21 E-mail: ktorigoe@nagasaki-u.ac.jp

22

23 Key words: Peritoneal dialysis, peritoneal fibrosis, mitochonic acid-5,

24 chlorhexidine gluconate

Abstract

Purpose: Peritoneal fibrosis is a serious complication of long-term peritoneal dialysis, attributable to inflammation and mitochondrial dysfunction. Mitochonic acid-5 (MA-5), an indole-3-acetic acid derivative, improves mitochondrial dysfunction and has therapeutic potential against various diseases including kidney diseases. However, whether MA-5 is effective against peritoneal fibrosis remains unclear. Therefore, we investigated the effect of MA-5 using a peritoneal fibrosis mouse model.

Methods: Peritoneal fibrosis was induced in C57BL/6 mice via intraperitoneal injection of chlorhexidine gluconate (CG) every other day for 3 weeks. MA-5 was administered daily by oral gavage. The mice were divided into control, MA-5, CG, and CG + MA-5 groups. Following treatment, immunohistochemical analyses were performed.

Results: Fibrotic thickening of the parietal peritoneum induced by CG was substantially attenuated by MA-5. The number of α-smooth muscle actin-positive myofibroblasts, transforming growth factor β-positive cells, F4/80-positive macrophages, monocyte chemotactic protein 1-positive cells, and 4-hydroxy-2-nonenal-positive cells was considerably decreased. In addition,

reduced ATP5a1-positive and uncoupling protein 2-positive cells in the CG group were notably increased by MA-5.

Conclusions: MA-5 may ameliorate peritoneal fibrosis by suppressing macrophage infiltration and oxidative stress, thus restoring mitochondrial function. Overall, MA-5 has therapeutic potential against peritoneal fibrosis.

Introduction

Peritoneal dialysis (PD) is a well-established treatment for end-stage renal disease. However, long-term PD leads to histopathological changes in the peritoneum, such as peritoneal fibrosis, which is attributed to increased collagen accumulation and myofibroblast proliferation with inflammatory cell infiltration in submesothelial areas [1–3]. In particular, peritoneal fibrosis leads to decreased PD effectiveness and ultrafiltration failure, resulting in PD withdrawal [4]. Moreover, peritoneal fibrosis can progress to encapsulating peritoneal sclerosis resulting in high mortality; it is one of the most critical complications of PD [5]. Recently, oxidative stress has been reported to play an important role in peritoneal injury, including fibrosis [6]. However, the precise mechanism of peritoneal fibrosis in patients with PD remains unclear, and no specific treatment has been established.

Mitochondrial dysfunction causes increased oxidative stress and plays an important role in fibrosis in organs such as the lungs [7, 8], liver [9, 10], and kidneys [11] by increasing the production of cytokines, such as transforming growth factor β (TGF-β), by macrophages and the activation of myofibroblasts.

Additionally, mitochondrial dysfunction contributes to peritoneal fibrosis by increasing oxidative stress [6, 12–14].

Mitochonic acid 5 (MA-5), 4-(2,4-difluorophenyl)-2-(1H-indol-3-yl)-4-oxobutanoic acid, is a newly-identified mitochondria-homing drug. MA-5 is a derivative of indole-3-acetic acid (IAA), which is a plant hormone auxin and accumulates in patients with renal failure [15]. MA-5 facilitates mitochondrial ATP production and reduces oxidative stress in fibroblasts from patients with mitochondrial diseases [16]. Moreover, MA-5 has therapeutic potential against mitochondrial dysfunction in kidney disease models [17]. Based on these results, we predicted that MA-5 may ameliorate peritoneal fibrosis by improving mitochondrial dysfunction. Therefore, our aim was to investigate the effect of MA-5 in a peritoneal fibrosis mouse model induced by chlorhexidine gluconate (CG).

Materials and Methods

Materials

MA-5 was provided by Dr. T. Abe (Tohoku University Graduate School of Medicine, Sendai, Japan) and was dissolved in 0.2 mL distilled water to obtain a final concentration of 0.25 mg/mL (2 mg/kg). We started administering MA-5 at a low dose of 2 mg/kg, and as the antifibrotic effect was confirmed and no adverse events such as liver damage were observed, we set the concentration to 2 mg/kg. CG solution was purchased from Dainippon Sumitomo Pharma (Osaka, Japan) and diluted to 0.05% with 15% ethanol in saline.

Animals

Ten-week-old male C57BL/6 mice weighing 24–29 g (Japan SLC Inc., Shizuoka, Japan) were used in this study. They were housed in standard rodent cages in a light- and temperature-controlled room at the Biomedical Research Center, Center for Frontier Life Sciences, Nagasaki University (Nagasaki, Japan). They had free access to pelleted rodent food and drinking water. The experimental protocol was approved by the Ethics Review Committee for Animal Experimentation of Nagasaki University School of Medicine (approval number 1506261242-7).

103

104 **Animal experimental protocol**

105

106 Peritoneal fibrosis was induced via the intraperitoneal injection of 0.05% CG in
107 15% ethanol dissolved in saline, as described previously, with a slight
108 modification [18, 19]. The mice were injected with CG into the peritoneal cavity
109 at a volume of 10 mL/kg every other day. When injecting CG into the peritoneal
110 cavity, the needle was inserted into the lateral abdomen of the mice. The
111 peritoneal tissues were collected from the midline part. The collected peritoneal
112 tissues were not affected by the needle prick. MA-5 was administered orally
113 every day at a concentration of 2 mg/kg from the time of the initial CG injection.
114 The mice were divided into four groups: control (CTL), in which 15% ethanol
115 dissolved in saline was injected intraperitoneally, and the vehicle was
116 administered orally (n = 5); MA-5, in which 15% ethanol dissolved in saline was
117 injected intraperitoneally, and MA-5 was administered orally (n = 5); CG, in
118 which CG was injected intraperitoneally, and the vehicle was administered orally
119 (n = 8); and CG + MA-5, in which CG was injected intraperitoneally, and MA-5
120 was administered orally (n = 8). Twenty-one days after the first administration,

the mice were sacrificed, and the peritoneal tissues were dissected.

Histological and immunohistochemical analyses

The peritoneal tissues were fixed in 4% paraformaldehyde in phosphate-buffered saline (PBS; pH 7.4) immediately after sampling and embedded in paraffin for histological examination and immunohistochemistry. For morphological examination, 4-μm-thick paraffin-embedded tissues were stained with Masson's trichrome stain. The following antibodies were used for immunohistochemistry: rabbit anti-type III collagen (1:400; LB-1393; LSL Co., Tokyo, Japan); rabbit anti- TGF-β (1:25; sc-146; Santa Cruz Biotechnology, Santa Cruz, CA); mouse anti-α-smooth muscle actin (α-SMA; 1:50; A2547; Sigma-Aldrich, St. Louis, MO), which was used as a myofibroblast marker; rat anti-F4/80 (1:50; MCA497; Bio-Rad, Hercules, CA), which was used as a macrophage marker; goat anti-monocyte chemotactic protein 1 (MCP1; 1:200; sc-1784; Santa Cruz Biotechnology); rabbit anti-CD31 (1:1000; ab182981; Abcam, Cambridge, UK), which was used as a vessel marker; mouse anti-4-hydroxy-2-nonenal (4-HNE; 1:50; MHN-100P; JaICA, Shizuoka, Japan), which was used as an oxidative

stress marker; rabbit anti-superoxide dismutase 2 (SOD2; 1:100; ab13534, Abcam), which was used as an antioxidant marker; rabbit anti-ATP5a1 (1:50; A5884; ABclonal, Woburn, MA); and uncoupling protein 2 (UCP2; 1:50; ab203244, Abcam), which was used as a mitochondrial expression marker.

After deparaffinization, the sections were treated with proteinase K (P2308; Sigma-Aldrich) for 15 min at 37 °C for antigen retrieval for type III collagen, TGF-β, α-SMA, F4/80, MCP1, and UCP2 staining. For CD31, 4-HNE, SOD2, and ATP5a1 staining, the sections were heated to 95 °C for 15 min in 10 mM citrate buffer (pH 6.0) for antigen retrieval. The sections were treated with 0.3% H_2O_2 in methanol for 20 min to inactivate endogenous peroxidase activity and then incubated with a blocking solution (Protein Block Serum-Free [X0909; Dako, Carpinteria, CA], 10% normal goat serum, or 10% normal rabbit serum) for 30 min at room temperature (RT). The sections were then incubated with the primary antibody diluted in the blocking solution for 1 h at RT (type III collagen, α-SMA, and MCP1) or overnight at 4 °C (TGF-β, F4/80, CD31, 4-HNE, SOD2, ATP5a1, and UCP2). For type III collagen staining, the sections were treated with the primary antibody for 1 h at RT followed by incubation with horseradish peroxidase (HRP)-conjugated swine anti-rabbit immunoglobulin antibody

157 (P0399; Dako) diluted at 1:50 for 30 min at RT. The sections were reacted with
158 the avidin-biotin complex using appropriate VECTASTAIN Elite ABC Kits (PK-
159 6101 for TGF-β staining or PK-6105 for MCP1 staining; Vector Laboratories,
160 Burlingame, CA) after incubation with the primary antibody for TGF-β staining
161 and MCP1 staining, respectively. For α-SMA staining, the sections were stained
162 using the rabbit EnVision kit (K4002; Dako) with a complex of the primary
163 antibody and HRP-conjugated rabbit anti-mouse immunoglobulin antibody
164 (P0161; Dako) for 1 h at RT. For F4/80 staining, the sections were treated with
165 the primary antibody overnight at 4 °C, and HRP-conjugated rabbit anti-rat
166 immunoglobulin antibody (P0450; Dako) diluted to 1:100 ratio for 30 min at RT
167 and then incubated with HRP-conjugated swine anti-rabbit immunoglobulin
168 antibody (P0399; Dako) diluted to 1:50 ratio for 30 min at RT. For CD31
169 staining, after treating the sections with the primary antibodies overnight at 4 °C,
170 they were incubated with the rabbit EnVision kit (K4003; Dako) for 1 h at RT.
171 For 4-HNE, SOD2, ATP5a1, and UCP2 staining, after treating the sections with
172 the primary antibodies overnight at 4 °C, they were incubated with HRP-
173 conjugated goat anti-mouse immunoglobulin antibody (P0447; Dako) diluted to
174 1:50 ratio or goat anti-rabbit immunoglobulin antibody (P0448; Dako) diluted to

1:200 ratio for 1 h at RT. After each reaction, the sections were washed with PBS. The reaction products were visualized by treating the sections with hydrogen peroxide and 3,3-diaminobenzidine tetrahydrochloride. Finally, after counterstaining with methyl green, the sections were dehydrated and mounted. For all specimens, negative controls were prepared using normal IgG instead of the primary antibody.

Immunofluorescence staining

The peritoneal tissues were fixed in 4% paraformaldehyde in PBS (pH 7.4) immediately after sampling and embedded in paraffin for immunofluorescence staining. The primary antibodies used for immunohistochemistry were as follows: mouse anti-4-HNE (1:50; MHN-100P; JaICA) and UCP2 (1:100; ab203244; Abcam). After deparaffinization, the sections were heated to 95 °C for 15 min in 10 mM citrate buffer (pH 6.0) for antigen retrieval. The sections were incubated with a blocking solution (Protein Block Serum-Free [X0909; Dako]) for 60 min at RT. The sections were then incubated with the primary antibodies diluted in the blocking solution overnight at 4 °C. The sections were incubated

with the following secondary antibodies for 1 h: Alexa Fluor dye (Molecular Probes Inc., Eugene, OR), 488-labeled goat anti-mouse IgG (A11001; Invitrogen, Paisley, UK) for 4-HNE staining, or Alexa Fluor dye 594-labeled goat anti-rabbit IgG (A11012; Invitrogen) for UCP2 staining. After each reaction, the sections were washed with PBS. Finally, after counterstaining with 4′,6-diamidino-2-phenylindole (DAPI), the sections were dehydrated and mounted. The sections were analyzed using a fluorescence microscope (BZ-X710; KEYENCE, Osaka, Japan). For all specimens, negative controls were prepared using normal IgG instead of the primary antibody.

Histological analysis

To perform semiquantitative analysis of the morphological changes in the peritoneum, we used digitized images and image analysis software (WinROOF2018; Mitani Corporation, Fukui, Japan). We measured the thickness of the submesothelial compact zone above the abdominal muscle in cross-sections of the abdominal wall. The image was transformed into a matrix of 1440 × 1024 pixels and viewed at 200× or 400× magnification using a light

211 microscope (Nikon ECLIPSE Ci-L; Nikon, Tokyo, Japan). Five different regions
212 were randomly selected, and the thickness of the submesothelial compact zone
213 was measured by Masson's trichrome staining. In each peritoneal sample, the
214 type III collagen-positive area was calculated in five fields at 200×
215 magnification. The cells that were positive for TGF-β, α-SMA, F4/80, MCP1, 4-
216 HNE, SOD2, ATP5a1, and UCP2 were counted in five fields at 200× or 400×
217 magnification. For SOD2, ATP5a1, and UCP2, the proportion of positive cells
218 among all cells in the submesothelial compact zone per field was calculated. The
219 CD31-positive vessels were counted in five fields at 200× magnification.
220
221 **Peritoneal equilibration test (PET)**
222
223 The peritoneal equilibration test (PET) was performed just before the sacrifice on
224 day 21. Eight milliliters of 2.5% Reguneal solution (ATB3627; Baxter Japan,
225 Tokyo, Japan) was injected into the abdominal cavity of mice. After 1 h, the
226 peritoneal effluent was collected. Blood samples were obtained from the inferior
227 vena cava immediately after the PET. Creatinine levels of peritoneal effluent and
228 serum were measured at SRL, Inc. (Tokyo, Japan). The dialysate-to-serum (D/S)

ratio of creatinine was calculated.

Quantification of proteins by enzyme-linked immunosorbent assay (ELISA)

Protein concentration in PD effluent and serum was measured using an enzyme-linked immunosorbent assay (ELISA) for 8-hydroxy-2'-deoxyguanosine (8-OHdG; KOG-HS10/E; JaICA). Optical density was measured using a microplate reader (Synergy LX Multi-Mode Microplate Reader; BioTek, Winooski, VT).

Statistical analyses

Data are expressed as mean ± standard error. Differences among the groups were examined for statistical significance using repeated measures analysis of variance (Tukey's honest significant difference test). Statistical significance was set at $p < 0.05$. All statistical analyses were performed using JMP version 15 software (SAS Institute Inc., Cary, NC).

Results

247

248 **MA-5 attenuates peritoneal fibrotic thickening induced by CG**

249

250 To assess the effect of MA-5 on peritoneal fibrotic thickening induced by CG, we
251 performed Masson's trichrome staining (Fig. 1a–e). In the CTL group, the
252 surface of the peritoneal tissue was covered with a monolayer of mesothelial
253 cells but displayed no thickening of the submesothelial compact zone (Fig. 1a).
254 In the MA-5 group, the peritoneum was not affected by the administration of
255 MA-5 and was similar to that in the CTL group (Fig. 1b) (14.1 vs. 21.0 μm, p =
256 0.90). However, the peritoneal tissues in the CG group showed considerable
257 thickening of the submesothelial compact zone (Fig. 1c) (93.8 vs. 21.0 μm, $p <$
258 0.0001). Additionally, the thickness of the submesothelial compact zone in the
259 CG + MA-5 group was significantly lower than that in the CG group (Fig. 1d)
260 (66.5 vs. 93.8 μm, $p = 0.0092$).

261 Further, we performed immunohistochemistry of type III collagen to analyze
262 collagen deposition (Fig. 1f–i). In the CG group, type III collagen was diffusely
263 expressed, and the positive area was significantly larger than that in the CTL
264 group (Fig. 1f, g) (198.3 vs. 27.8 μm^2, $p < 0.0001$). Type III collagen-positive

area in the CG + MA-5 group (Fig. 1h) was significantly reduced compared with that in the CG group (110.6 vs. 198.3 μm^2, $p = 0.0022$).

These results indicate that MA-5 has an antifibrotic effect on peritoneal fibrosis induced by CG.

Furthermore, we evaluated peritoneal permeability by performing PET (Online Resource 1). The D/S ratio of creatinine in the CG group was significantly higher than that in the CTL group (0.76 vs. 0.46, $p = 0.0091$). However, the D/S ratio of creatinine in the CG + MA-5 group was lower than that in the CG group, although the difference was not statistically significant (0.70 vs. 0.76, $p = 0.76$). These results, consistent with the results of the histological analysis, suggest that MA-5 may attenuate the peritoneal hyperpermeability of our CG-induced peritoneal fibrosis mouse model.

MA-5 attenuates fibrosis by suppressing TGF-β and α-SMA

As TGF-β is known to be a crucial factor in the development of fibrosis, we examined the number of TGF-β-positive cells in the peritoneal tissues using immunohistochemistry (Fig. 2a–d). In the CTL group, a few TGF-β-positive cells

were found in the submesothelial zone (Fig. 2a, e). In the CG group, numerous TGF-β-positive cells were observed in the thickened peritoneum (Fig. 2b, f) (226.5 vs. 23.1 cells/field, $p = 0.021$), whereas TGF-β-positive cells were significantly reduced in the CG + MA-5 group (Fig. 2c, g) compared with those in the CG group (69.8 vs. 226.5 cells/field, $p = 0.0089$).

Furthermore, we evaluated the expression of α-SMA, which is a marker of myofibroblasts in peritoneal tissues (Fig. 2h–n). In the CTL group, the number of α-SMA-positive cells was low in the submesothelial zone (Fig. 2h, l). On the contrary, in the CG group, numerous α-SMA-positive cells accumulated in the thickened peritoneum, especially in the upper layer (Fig. 2i, m) (281.3 vs. 29.7 cells/field, $p = 0.0023$), whereas the number of α-SMA-positive cells was significantly decreased in the CG + MA-5 group (Fig. 2j, n) compared with that in the CG group (116.3 vs. 281.3 cells/field, $p = 0.015$).

These results indicate that MA-5 suppressed TGF-β expression and α-SMA-positive myofibroblast proliferation in the peritoneum in our CG-induced peritoneal fibrosis mouse model.

MA-5 ameliorates macrophage infiltration and MCP1 expression

CG induces peritoneal fibrosis via macrophage infiltration [20]. Therefore, we investigated the degree of macrophage infiltration by performing immunohistochemistry for F4/80 as a marker for mouse macrophages in peritoneal tissues (Fig. 3a–g). In the CTL group, a small number of macrophages were found in the submesothelial zone (Fig. 3a, e). In the CG group, numerous macrophages were observed in the thickened peritoneum (Fig. 3b, f) (107.6 vs. 9.6 cells/field, $p < 0.0001$), whereas the number of macrophages was considerably reduced in the CG + MA-5 group (Fig. 3c, g) compared to that in the CG group (62.1 vs. 107.6 cells/field, $p = 0.0010$). We also investigated the expression of MCP1, which promotes macrophage infiltration (Fig. 3h–n). In the CTL group, a few MCP1-positive cells were found in the submesothelial zone (Fig. 3h, l). In the CG group, numerous MCP1-positive cells were detected in the thickened peritoneum (Fig. 3i, m) (262.4 vs. 20.7 cells/field, $p = 0.0011$), whereas MCP1-positive cells were considerably decreased in the CG + MA-5 group (Fig. 3j, n) compared with those in the CG group (96.7 vs. 262.4 cells/field, $p = 0.0062$).

These results suggest that MA-5 repressed the expression of MCP1 and

macrophage infiltration in the peritoneum of our CG-induced peritoneal fibrosis mouse model.

MA-5 suppresses angiogenesis

In our previous studies, we have shown that some drugs improved peritoneal fibrosis and reduced angiogenesis [21, 22]. Therefore, in this study, we evaluated angiogenesis by immunohistochemistry of CD31, a marker of vessels, in the peritoneal tissues (Fig. 4a–g). In the CTL group, no CD31-positive vessels were found in the submesothelial zone (Fig. 4a, e). On the contrary, in the CG group, several CD31-positive vessels were detected (Fig. 4b, f) (17.4 vs. 0.0 vessels/field, $p < 0.0001$), whereas CD31-positive vessels were significantly decreased in the CG + MA-5 group (Fig. 4c, g) compared with those in the CG group (6.4 vs. 17.4 vessels/field, $p = 0.0010$). These results indicate that MA-5 suppressed angiogenesis in the peritoneum of our CG-induced peritoneal fibrosis mouse model.

MA-5 decreases oxidative stress

337

338 4-HNE is a natural byproduct of lipid peroxidation, which generally reflects
339 oxidative stress [12]. Therefore, we evaluated the oxidative stress level in
340 peritoneal tissues by immunohistochemistry for 4-HNE (Fig. 5a–g). In the CTL
341 group, a few 4-HNE-positive cells were found in the submesothelial zone (Fig.
342 5a, e). In the CG group, numerous 4-HNE-positive macrophages and
343 myofibroblasts were observed in the thickened peritoneum (Fig. 5b, d, f) (75.3
344 vs. 0.7 cells/field, $p < 0.0001$), whereas 4-HNE-positive cells were significantly
345 reduced in the CG + MA-5 group (Fig. 5c, g), compared with those in the CG
346 group (45.5 vs. 75.3 cells/field, $p = 0.0051$). These results suggest that MA-5
347 may reduce peritoneal oxidative stress induced by CG.
348 Additionally, we measured the concentration of 8-OHdG, one of the oxidative
349 stress markers, in peritoneal effluent and serum (Online Resource 2). No
350 significant difference in the 8-OHdG concentration in both peritoneal effluent
351 (0.13 vs. 0.22 ng/mL, $p = 0.48$; 0.22 vs. 0.19 ng/mL, $p = 0.87$) and serum (0.20
352 vs. 0.24 ng/mL, $p = 0.99$; 0.24 vs. 0.80 ng/mL, $p = 0.051$) between the CTL and
353 the CG groups and the CG and the CG + MA-5 groups was observed. These
354 results indicated that the effect of MA-5 could be limited to the peritoneal region.

Moreover, we performed immunohistochemistry of SOD2 to evaluate antioxidant capacity (Online Resource 3). There was no significant difference in the proportion of SOD2-positive cells in the submesothelial zone (74.0% vs. 79.7%, $p = 0.53$; 79.7% vs. 81.5%, $p = 0.92$) between the CTL (Online Resource 3a) and the CG group (Online Resource 3b) and the CG and CG + MA-5 groups (Online Resource 3c). These results suggested that MA-5 might not be involved in the antioxidant capacity of the peritoneum.

MA-5 restores the decreased expression of mitochondrial components

Mitochondrial dysfunction has been reported to cause peritoneal fibrosis via increased oxidative stress [6, 12–14], and MA-5 recovers mitochondrial function by reducing oxidative stress in kidney tissues and cardiac myocytes [18]. Therefore, we assessed the mitochondrial component expression level in the peritoneal tissues by performing immunohistochemistry of ATP5a1 and UCP2, both of which play an important role in mitochondrial function (Fig. 6a–g). In the CTL group, ATP5a1 and UCP2 expression was preserved in the submesothelial zone, mainly in mesothelial cells (Fig. 6a, e). However, in the CG group, the

proportion of positive cells for ATP5a1 and UCP2 was lower than that in the CTL group (Fig. 6b, f) (58.3% vs. 83.5%, $p = 0.0006$; 54.2% vs. 89.5%, $p < 0.0001$). Meanwhile, the decreased proportion of positive cells for ATP5a1 and UCP2 was restored in the CG + MA-5 group mainly in myofibroblasts and macrophages (Fig. 6c, g) (74.2% vs. 58.3%, $p = 0.011$; 87.3% vs. 54.2 %, $p < 0.0001$). These results suggest that MA-5 may ameliorate mitochondrial dysfunction in the peritoneum of our CG-induced peritoneal fibrosis mouse model.

Moreover, we performed double immunofluorescence staining of 4-HNE and UCP2 (Fig. 7a–c). In the CTL group, most of the cells, the majority of which were mesothelial cells, were 4-HNE-negative and UCP2-positive (Fig. 7a). In the CG group, most of the cells that appeared to be myofibroblasts were 4-HNE-negative and UCP2-positive, whereas 4-HNE-positive and UCP2-negative cells were observed among the cells that appeared to be macrophages (Fig. 7b). In the CG + MA-5 group, myofibroblasts were similar to those in the CG group; however, 4-HNE-negative and UCP2-positive macrophages were increased compared with those in the CG group (Fig. 7c). These results suggest MA-5 treatment may reduce oxidative stress in cells with improved mitochondrial function, which appear to be mainly macrophages.

Discussion

In this study, we demonstrate that MA-5 considerably attenuated CG-induced peritoneal fibrosis by reducing the number of myofibroblasts in mice. Furthermore, this antifibrotic effect was accompanied by a decrease in macrophage infiltration. We also showed that oxidative stress was reduced, and mitochondrial function was restored by treatment with MA-5. These findings suggest that MA-5 is beneficial for preventing the progression of peritoneal fibrosis.

Macrophage infiltration is involved in CG-induced peritoneal fibrosis [19]. In the present study, we observed that MA-5 reduced macrophage infiltration into the peritoneum. Moreover, MA-5 suppressed MCP1 expression of myofibroblasts and macrophages in the peritoneum. MCP1 has been shown to play an important role in the initiation and progression of peritoneal fibrosis via the recruitment and activation of macrophages, which secrete profibrotic cytokines, such as TGF-β [20, 23]. Thus, our results suggest that MA-5 ameliorates peritoneal fibrosis by repressing macrophage infiltration and TGF-β

409 expression via the suppression of MCP1 expression. Furthermore, MA-5 reduced
410 CD31-positive vessels in the peritoneum, suggesting that MA-5 also has anti-
411 angiogenic effects accompanied by its antifibrotic effects.
412 Oxidative stress triggers inflammatory conditions, including macrophage
413 infiltration in the peritoneum, and mitochondria are a major site for the
414 production of reactive oxygen species (ROS) [6, 14, 24, 25]. As for the
415 mechanism of the effects of MA-5 on mitochondria, previous studies have shown
416 that MA-5 binds to mitofilin, an inner mitochondrial membrane protein, and
417 induces ATP synthase oligomerization, supercomplex formation, and a
418 conformational change in cristae [26]. These improvements in mitochondrial
419 morphology and dynamics promote effective ATP synthesis without generating
420 mitochondrial ROS [26]. In addition, it has been reported that supercomplex
421 formation prevents excessive mitochondrial ROS production [27]. Furthermore,
422 the proportion of ATP5a1- and UCP2-positive cells in myofibroblasts and
423 macrophages was restored in our study. The number of 4-HNE-positive
424 myofibroblasts and macrophages was reduced in the CG + MA-5 group
425 compared with that in the CG group, suggesting that MA-5 treatment recovered
426 mitochondrial function and reduced oxidative stress in cells comprising the

peritoneal submesothelial compact zone. The double immunofluorescence staining for 4-HNE and UCP2 showed that 4-HNE-negative and UCP2-positive macrophages in the CG + MA-5 group increased compared with those in the CG group, suggesting that MA-5 treatment improved the mitochondrial function of macrophages mainly and reduced oxidative stress.

These results indicate that MA-5 can inhibit peritoneal fibrosis by suppressing inflammation, including macrophage infiltration, via the reduction of oxidative stress by restoring mitochondrial function.

Although our results show the beneficial effects of MA-5 treatment, our study has some limitations. First, we used a CG-induced peritoneal fibrosis mouse model, but CG may not imitate human peritoneal fibrosis. Nevertheless, the CG model can be regarded as an important experimental model because the histological changes, including myofibroblast proliferation and macrophage infiltration in the CG model, were similar to those of peritoneal fibrosis in PD patients. These similarities strongly indicate that the CG model is suitable for studying the pathogenesis and treatment of peritoneal fibrosis. Second, MA-5 and CG were administered simultaneously. The effects of MA-5 as a therapeutic intervention after CG initiation have not been determined. Therefore, the

therapeutic efficacy of MA-5 requires further investigation. Finally, in our study, the direct causal relationship between MA-5 and the restoration of mitochondrial function and morphology was not elucidated. However, it has been confirmed by electron microscopy that mitochondrial cristae enlarged and shortened by mitochondrial damage become thinner and longer with MA-5 administration [26]. Further studies are needed to establish the protective mechanism of MA-5.

Conclusions

We demonstrate that MA-5 can ameliorate peritoneal fibrosis in a CG-induced peritoneal fibrosis mouse model. Our results indicate that the antifibrotic effect of MA-5 may involve the suppression of macrophage infiltration via the recovery of mitochondrial function and reduction in oxidative stress. Thus, MA-5 constitutes a novel treatment option for the prevention of peritoneal fibrosis.

CONFLICT OF INTEREST

The authors declare that they have no conflicts of interest.

FUNDING

This work was supported in part by a National Grant-in-Aid for Scientific Research from the Ministry of Education, Culture, Sports, Science, and Technology of Japan (18H02822(TA)) and Japan Agency for Medical Research and Development (AMED) J21000294.

ACKNOWLEDGMENTS

We would like to thank Ms. Ryoko Yamamoto for her excellent experimental assistance.

References

1. Gandhi VC, Humayun HM, Ing TS, Daugirdas JT, Jablokow VR, Iwatsuki S, Geis WP, Hano JE (1980) Sclerotic thickening of the peritoneal membrane in maintenance peritoneal dialysis patients. Arch Intern Med 140:1201–1203. https://doi.org/10.1001/archinte.1980.00330200077024
2. Williams JD, Craig KJ, Topley N, Von Ruhland C, Fallon M, Newman GR, Mackenzie RK, Williams GT, Peritoneal Biopsy Study Group (2002) Morphologic changes in the peritoneal membrane of patients with renal disease. J Am Soc Nephrol 13:470–479. https://doi.org/10.1681/ASN.V132470
3. Zhang Z, Jiang N, Ni Z (2017) Strategies for preventing peritoneal fibrosis in peritoneal dialysis patients: New insights based on peritoneal inflammation and angiogenesis. Front Med 11:349–358. https://doi.org/10.1007/s11684-017-0571-2
4. Kawaguchi Y, Ishizaki T, Imada A, Oohira S, Kuriyama S, Nakamoto H, Nakamoto M, Hiramatu M, Maeda K, Ota K, Study Group for Withdrawal from PD in Japan (2003) Searching for the reasons for drop-out from peritoneal dialysis: A nationwide survey in Japan. Perit Dial Int 23

492 Supplement 2:S175-7. https://doi.org/10.1177/089686080302302s36:S175–
493 S177
494 5. Nakayama M, Miyazaki M, Honda K, Kasai K, Tomo T, Nakamoto H,
495 Kawanishi H (2014) Encapsulating peritoneal sclerosis in the era of a multi-
496 disciplinary approach based on biocompatible solutions: The next-PD study.
497 Perit Dial Int 34:766–774. https://doi.org/10.3747/pdi.2013.00074
498 6. Roumeliotis S, Dounousi E, Salmas M, Eleftheriadis T, Liakopoulos V
499 (2020) Unfavorable effects of peritoneal dialysis solutions on the peritoneal
500 membrane: The role of oxidative stress. Biomolecules 10:768.
501 https://doi.org/10.3390/biom10050768
502 7. Rangarajan S, Bernard K, Thannickal VJ (2017) Mitochondrial dysfunction
503 in pulmonary fibrosis. Ann Am Thorac Soc 14:S383–S388.
504 https://doi.org/10.1513/AnnalsATS.201705-370AW
505 8. Mora AL, Bueno M, Rojas M (2017) Mitochondria in the spotlight of aging
506 and idiopathic pulmonary fibrosis. J Clin Invest 127:405–414.
507 https://doi.org/10.1172/JCI87440
508 9. Pérez-Carreras M, del Hoyo P, Martín MA, Rubio JC, Martín A, Castellano
509 G, Colina F, Arenas J, Solis-Herruzo JA (2003) Defective hepatic

510 mitochondrial respiratory chain in patients with nonalcoholic steatohepatitis.
511 Hepatology 38:999–1007. https://doi.org/10.1053/jhep.2003.50398
512 10. Paradies G, Paradies V, Ruggiero FM, Petrosillo G (2014) Oxidative stress,
513 cardiolipin and mitochondrial dysfunction in nonalcoholic fatty liver disease.
514 World J Gastroenterol 20:14205–14218.
515 https://doi.org/10.3748/wjg.v20.i39.14205
516 11. Xinyu Li, Wei Zhang, Qingtai Cao, Zeyu Wang, Mingyi Zhao, Linyong Xu,
517 Quan Zhuangcorresponding (2020) Mitochondrial dysfunction in fibrotic
518 diseases. Cell Death Discov 6: 80. https://doi.org/10.1038/s41420-020-
519 00316-9
520 12. Shin HS, Ko J, Kim DA, Ryu ES, Ryu HM, Park SH, Kim YL, Oh ES, Kang
521 DH (2017) Metformin ameliorates the phenotype transition of peritoneal
522 mesothelial cells and peritoneal fibrosis via a modulation of oxidative stress.
523 Sci Rep 7:5690. https://doi.org/10.1038/s41598-017-05836-6
524 13. Hung KY, Liu SY, Yang TC, Liao TL, Kao SH (2014) High-dialysate-
525 glucose-induced oxidative stress and mitochondrial-mediated apoptosis in
526 human peritoneal mesothelial cells. Oxid Med Cell Longev 2014:642793.
527 https://doi.org/10.1155/2014/642793

14. Lu H, Chen W, Liu W, Si Y, Zhao T, Lai X, Kang Z, Sun X, Guo Z (2020) Molecular hydrogen regulates PTEN-AKT-mTOR signaling via ROS to alleviate peritoneal dialysis-related peritoneal fibrosis. FASEB J 34:4134–4146. https://doi.org/10.1096/fj.201901981R

15. Toyohara T, Akiyama Y, Suzuki T, Takeuchi Y, Mishima E, Tanemoto M, Momose A, Toki N, Sato H, Nakayama M, Hozawa A, Tsuji I, Ito S, Soga T, Abe T (2010) Metabolomic profiling of uremic solutes in CKD patients. Hypertens Res 33:944–952. https://doi.org/10.1038/hr.2010.113

16. Suzuki T, Yamaguchi H, Kikusato M, Matsuhashi T, Matsuo A, Sato T, Oba Y, Watanabe S, Minaki D, Saigusa D, Shimbo H, Mori N, Mishima E, Shima H, Akiyama Y, Takeuchi Y, Yuri A, Kikuchi K, Toyohara T, Suzuki C, Kohzuki M, Anzai J, Mano N, Kure S, Yanagisawa T, Tomioka Y, Toyomizu M, Ito S, Osaka H, Hayashi K, Abe T (2015) Mitochonic acid 5 (MA-5), a derivative of the plant hormone indole-3-acetic acid, improves survival of fibroblasts from patients with mitochondrial diseases. Tohoku J Exp Med 236:225–232. https://doi.org/10.1620/tjem.236.225

17. Suzuki T, Yamaguchi H, Kikusato M, Hashizume O, Nagatoishi S, Matsuo A, Sato T, Kudo T, Matsuhashi T, Murayama K, Ohba Y, Watanabe S, Kanno S,

546 Minaki D, Saigusa D, Shinbo H, Mori N, Yuri A, Yokoro M, Mishima E,
547 Shima H, Akiyama Y, Takeuchi Y, Kikuchi K, Toyohara T, Suzuki C,
548 Ichimura T, Anzai J, Kohzuki M, Mano N, Kure S, Yanagisawa T, Tomioka
549 Y, Toyomizu M, Tsumoto K, Nakada K, Bonventre JV, Ito S, Osaka H,
550 Hayashi K, Abe T (2016) Mitochonic acid 5 binds mitochondria and
551 ameliorates renal tubular and cardiac myocyte damage. J Am Soc Nephrol
552 27:1925–1932. https://doi.org/10.1681/ASN.2015060623
553 18. Mishima Y, Miyazaki M, Abe K, Ozono Y, Shioshita K, Xia Z, Harada T,
554 Taguchi T, Koji T, Kohno S (2003) Enhanced expression of heat shock
555 protein 47 in rat model of peritoneal fibrosis. Perit Dial Int 23:14–22.
556 https://doi.org/10.1177/089686080302300102
557 19. Nakazawa M, Obata Y, Nishino T, Abe S, Nakazawa Y, Abe K, Furusu A,
558 Miyazaki M, Koji T, Kohno S (2013) Involvement of leptin in the
559 progression of experimentally induced peritoneal fibrosis in mice. Acta
560 Histochem Cytochem 46:75–84. https://doi.org/10.1267/ahc.13005
561 20. Topley N, Liberek T, Davenport A, Li FK, Fear H, Williams J (1996)
562 Activation of inflammation and leukocyte recruitment into the peritoneal
563 cavity. Kidney International, Supplement.

21. Kitamura M, Nishino T, Obata Y, Furusu A, Hishikawa Y, Koji T, Kohno S (2012) Epigallocatechin gallate suppresses peritoneal fibrosis in mice. Chem Biol Interact 5:95–104. https://doi.org/10.1016/j.cbi.2011.11.002.

22. Io K, Nishino T, Obata Y, Kitamura M, Koji T, Kohno S (2015) SAHA Suppresses Peritoneal Fibrosis in Mice. Perit Dial Int 35:246–58. https://doi.org/10.3747/pdi.2013.00089.

23. Lee SH, Kang HY, Kim KS, Nam BY, Paeng J, Kim S, Li JJ, Park JT, Kim DK, Han SH, Yoo TH, Kang SW (2012) The monocyte chemoattractant protein-1 (MCP-1)/CCR2 system is involved in peritoneal dialysis-related epithelial-mesenchymal transition of peritoneal mesothelial cells. Lab Invest 92:1698–1711. https://doi.org/10.1038/labinvest.2012.132

24. Liakopoulos V, Roumeliotis S, Gorny X, Eleftheriadis T, Mertens PR (2017) Oxidative stress in patients undergoing peritoneal dialysis: A current review of the literature. Oxid Med Cell Longev 2017:3494867. https://doi.org/10.1155/2017/3494867

25. Indo HP, Davidson M, Yen HC, Suenaga S, Tomita K, Nishii T, Higuchi M, Koga Y, Ozawa T, Majima HJ (2007) Evidence of ROS generation by mitochondria in cells with impaired electron transport chain and

582 mitochondrial DNA damage. Mitochondrion 7:106–118.
583 https://doi.org/10.1016/j.mito.2006.11.026
584 26. Matsuhashi T, Sato T, Kanno SI, Suzuki T, Matsuo A, Oba Y, Kikusato M,
585 Ogasawara E, Kudo T, Suzuki K, Ohara O, Shimbo H, Nanto F, Yamaguchi
586 H, Saigusa D, Mukaiyama Y, Watabe A, Kikuchi K, Shima H, Mishima E,
587 Akiyama Y, Oikawa Y, Hsin-Jung HO, Akiyama Y, Suzuki C, Uematsu M,
588 Ogata M, Kumagai N, Toyomizu M, Hozawa A, Mano N, Owada Y, Aiba S,
589 Yanagisawa T, Tomioka Y, Kure S, Ito S, Nakada K, Hayashi KI, Osaka H,
590 Abe T (2017) Mitochonic acid-5 (MA-5) facilitates ATP synthase
591 oligomerization and cell survival in various mitochondrial diseases.
592 EBioMedicine 20:27–38. https://doi.org/10.1016/j.ebiom.2017.05.016
593 27. Maranzana E, Barbero G, Falasca AI, Lenaz G, Genova ML (2013)
594 Mitochondrial respiratory supercomplex association limits production of
595 reactive oxygen species from complex I. Antioxid Redox Signal 19:1469–
596 1480. https://doi.org/10.1089/ars.2012.4845
597

598 **Figure Legends**

599 **Fig. 1** Masson's trichrome staining of the peritoneum (a–e) and
600 immunohistochemical analysis of type III collagen in the peritoneum (f–i). (a, b)
601 In the CTL and MA-5 groups, the monolayer of mesothelial cells covered the
602 entire surface of the peritoneum without thickening of the submesothelial
603 compact zone. (c) The parietal peritoneal tissues of the CG group showed
604 considerable fibrotic thickening of the submesothelial compact zone and the
605 presence of numerous cells. (d) The CG + MA-5 group showed significantly less
606 thickening of the submesothelial area than the CG group. (e) The bar graph
607 shows the thickening of the submesothelial compact zone. (f) In the CTL group,
608 there was slight type III collagen deposition. (g) In the CG group, the type III
609 collagen-positive area significantly increased in the thickened peritoneum. (h) In
610 the CG + MA-5 group, the type III collagen-positive area significantly decreased
611 compared with that in the CG group. (i) The bar graph shows the type III
612 collagen-positive area. ** represents $p < 0.01$; *** represents $p < 0.001$; Tukey's
613 honest significant difference test. Original magnification 200×; bars indicate the
614 thickness of the submesothelial zone. CG = chlorhexidine gluconate; CTL =
615 control; MA-5 = mitochonic acid-5

616

617 **Fig. 2** Immunohistochemical analysis of TGF-β (a–g) and α-SMA (h–n) in the
618 peritoneum. (a, e) In the CTL group, minimal TGF-β expression was observed.
619 (b, f) In the CG group, TGF-β expression was significantly increased in the
620 thickened peritoneum compared with that in the CG group. (c, g) In the CG +
621 MA-5 group, TGF-β expression was significantly decreased compared with that
622 in the CG group. (d) The bar graph shows the number of TGF-β-positive cells at
623 200× magnification. (h, l) In the CTL group, a few α-SMA-positive cells were
624 observed. (i, m) In the CG group, the number of α-SMA-positive cells
625 significantly increased in the thickened peritoneum. (j, n) In the CG + MA-5
626 group, the number of α-SMA positive cells was significantly decreased compared
627 with that in the CG group. (h) The bar graph shows the number of α-SMA-
628 positive cells at 200× magnification. * represents $p < 0.05$; ** represents $p <$
629 0.01; Tukey's honest significant difference test. Original magnification 200× (a–
630 c, h–j) or 400× (e–g, l–n); bars indicate the thickness of the submesothelial zone.
631 α-SMA = α-smooth muscle actin; CG = chlorhexidine gluconate; CTL = control;
632 MA-5 = mitochonic acid-5; TGF-β = transforming growth factor β
633

Fig. 3 Immunohistochemical analysis for F4/80 (a–g) and MCP1 (h–n) in the peritoneum. (a, e) In the CTL group, a few F4/80-positive cells were observed. (b, f) In the CG group, the number of F4/80-positive cells was significantly increased in the thickened peritoneum. (c, g) In the CG + MA-5 group, the number of F4/80-positive cells significantly decreased compared with that in the CG group. (d) The bar graph shows the number of F4/80-positive cells at 200× magnification. (h, l) In the CTL group, minimal MCP1 expression was observed. (i, m) In the CG group, MCP1 expression was significantly increased in the thickened peritoneum compared with that in the CTL group. (j, n) In the CG + MA-5 group, MCP1 expression was significantly decreased compared with that in the CG group. (k) The bar graph shows the number of MCP1-positive cells at 200× magnification. * represents $p < 0.05$; ** represents $p < 0.01$; *** represents $p < 0.001$; Tukey's honest significant difference test. Original magnification 200× (a–c, h–j) or 400× (e–g, l–n); bars indicate the thickness of the submesothelial zone. CG = chlorhexidine gluconate; CTL = control; MA-5 = mitochonic acid-5; MCP1 = monocyte chemotactic protein 1.

Fig. 4 Immunohistochemical analysis for CD31 in the peritoneum. (a, e) In the

652 CTL group, no CD31-positive vessels were observed. (b, f) In the CG group, the
653 number of CD31-positive vessels was significantly increased in the thickened
654 peritoneum. (c, g) In the CG + MA-5 group, the number of CD31-positive
655 vessels significantly decreased compared with that in the CG group. (d) The bar
656 graph shows the number of CD31-positive vessels. ** represents $p < 0.01$; ***
657 represents $p < 0.001$; Tukey's honest significant difference test. Original
658 magnification 200× (a–c) or 400× (e–g); bars indicate the thickness of the
659 submesothelial zone. CTL = control; MA-5 = mitochonic acid-5; CG =
660 chlorhexidine gluconate. Arrows indicate CD31-positive vessels
661
662 **Fig. 5** Immunohistochemical analysis of 4-HNE (a–g) in the peritoneum. (a, e) In
663 the CTL group, minimal 4-HNE expression was observed. (b, f) In the CG group,
664 4-HNE expression significantly increased in the thickened peritoneum compared
665 with that in the CTL group. (c, g) In the CG + MA-5 group, 4-HNE expression
666 significantly decreased compared with that in the CG group. (d) The bar graph
667 shows the number of 4-HNE-positive cells at 200× magnification. ** represents
668 $p < 0.01$; *** represents $p < 0.001$; Tukey's honest significant difference test.
669 Original magnification 200× (a–c) or 400× (e–g); bars indicate the thickness of

670 the submesothelial zone. 4-HNE = 4-hydroxy-2-nonenal; CTL = control; MA-5 =
671 mitochonic acid-5; CG = chlorhexidine gluconate
672
673 **Fig. 6** Immunohistochemical analysis for ATP5a1 (a–d) and UCP2 (e–h) in the
674 peritoneum. (a) In the CTL group, ATP5a1 expression in the component cells was
675 preserved. (b) In the CG group, the proportion of ATP5a1-positive cells
676 significantly decreased in the thickened peritoneum compared with that in the
677 CTL group. (c) In the CG + MA-5 group, the decreased proportion of ATP5a1-
678 positive cells was significantly restored compared with that in the CG group. (d)
679 The bar graph shows the proportion of ATP5a1-positive cells. (e) In the CTL
680 group, the expression of UCP2 in the component cells was maintained. (f) In the
681 CG group, the proportion of UCP2-positive cells significantly reduced in the
682 thickened peritoneum. (g) In the CG + MA-5 group, the reduced proportion of
683 UCP2-positive cells was significantly recovered compared with that in the CG
684 group. (h) The bar graph shows the proportion of UCP2-positive cells. **
685 represents $p < 0.01$; *** represents $p < 0.001$; Tukey's honest significant
686 difference test. Original magnification 400×; bars indicate the thickness of the
687 submesothelial zone. UCP2 = uncoupling protein 2; CTL = control; MA-5 =

688 mitochonic acid-5; CG = chlorhexidine gluconate

689

690 **Fig. 7** Immunofluorescence staining of 4-HNE and UCP2 in the peritoneum. (a)
691 In the CTL group, most of the cells were 4-HNE-negative and UCP2-positive. (b)
692 In the CG group, most of the cells that appeared to be myofibroblasts were 4-
693 HNE-negative and UCP2-positive, and 4-HNE-positive and UCP2-negative cells
694 were observed among the cells that appeared to be macrophages. (c) In the CG +
695 MA-5 group, most of the cells that appeared to be myofibroblasts were 4-HNE-
696 negative and UCP2-positive, and 4-HNE-negative and UCP2-positive cells that
697 appeared to be macrophages were increased compared with those in the CG
698 group. Original magnification 400×; bars indicate the thickness of the
699 submesothelial zone. 4-HNE = 4-hydroxy-2-nonenal; UCP2 = uncoupling protein
700 2; DAPI = 4′,6-diamidino-2-phenylindole; CTL = control; MA-5 = mitochonic
701 acid-5; CG = chlorhexidine gluconate. Arrows indicate myofibroblasts, and
702 arrowheads indicate macrophages

703

704 **Online Resource 1** The results of the peritoneal equilibration test. The bar graph
705 shows the D/S ratio of creatinine. D/S ratio of creatinine in the CG group was

706 higher compared with that in the CTL group. The D/S ratio of creatinine in the
707 CG + MA-5 group was lower than that in the CG group, although the difference
708 was not statistically significant. ** represents $p < 0.01$. D/S = dialysate-to-serum;
709 CTL = control; MA-5 = mitochonic acid-5; CG = chlorhexidine gluconate
710
711 **Online Resource 2** The concentration of 8-OHdG in peritoneal effluent (a) and
712 serum (b). The bar graphs show the concentration of 8-OHdG. There was no
713 significant difference in the concentration of 8-OHdG both in peritoneal effluent
714 and serum among the groups. 8-OHdG = 8-hydroxy-2'-deoxyguanosine; CTL =
715 control; MA-5 = mitochonic acid-5; CG = chlorhexidine gluconate
716
717 **Online Resource 3** Immunohistochemical analysis for SOD2 in the peritoneum
718 (a–d). There was no significant difference in the proportion of SOD2-positive
719 cells in the submesothelial zone among the CTL group (a), the CG group (b), and
720 the CG + MA-5 group (c). (d) The bar graph shows the proportion of SOD2-
721 positive cells. Original magnification 400×; bars indicate the thickness of the
722 submesothelial zone. SOD2 = superoxide dismutase 2; CTL = control; MA-5 =
723 mitochonic acid-5; CG = chlorhexidine gluconate

Figure 1

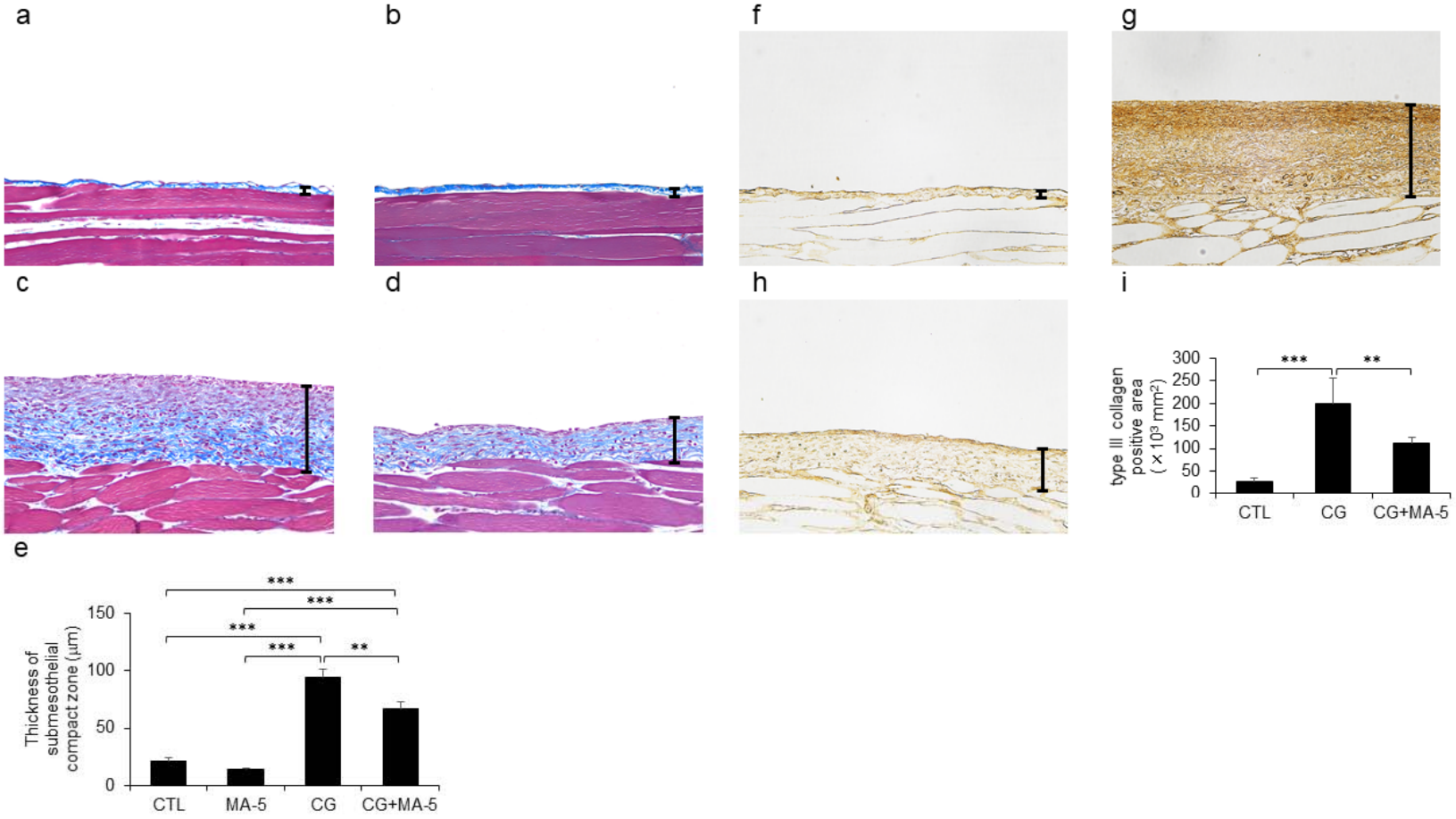
a
b
f
g
c
d
h
i
e
Thickness of submesothelial compact zone (μm)
150
100
50
0
***
***
***
***
**
CTL
MA-5
CG
CG+MA-5
type III collagen positive area (×10³ mm²)
300
250
200
150
100
50
0
***
**
CTL
CG
CG+MA-5

Figure 2

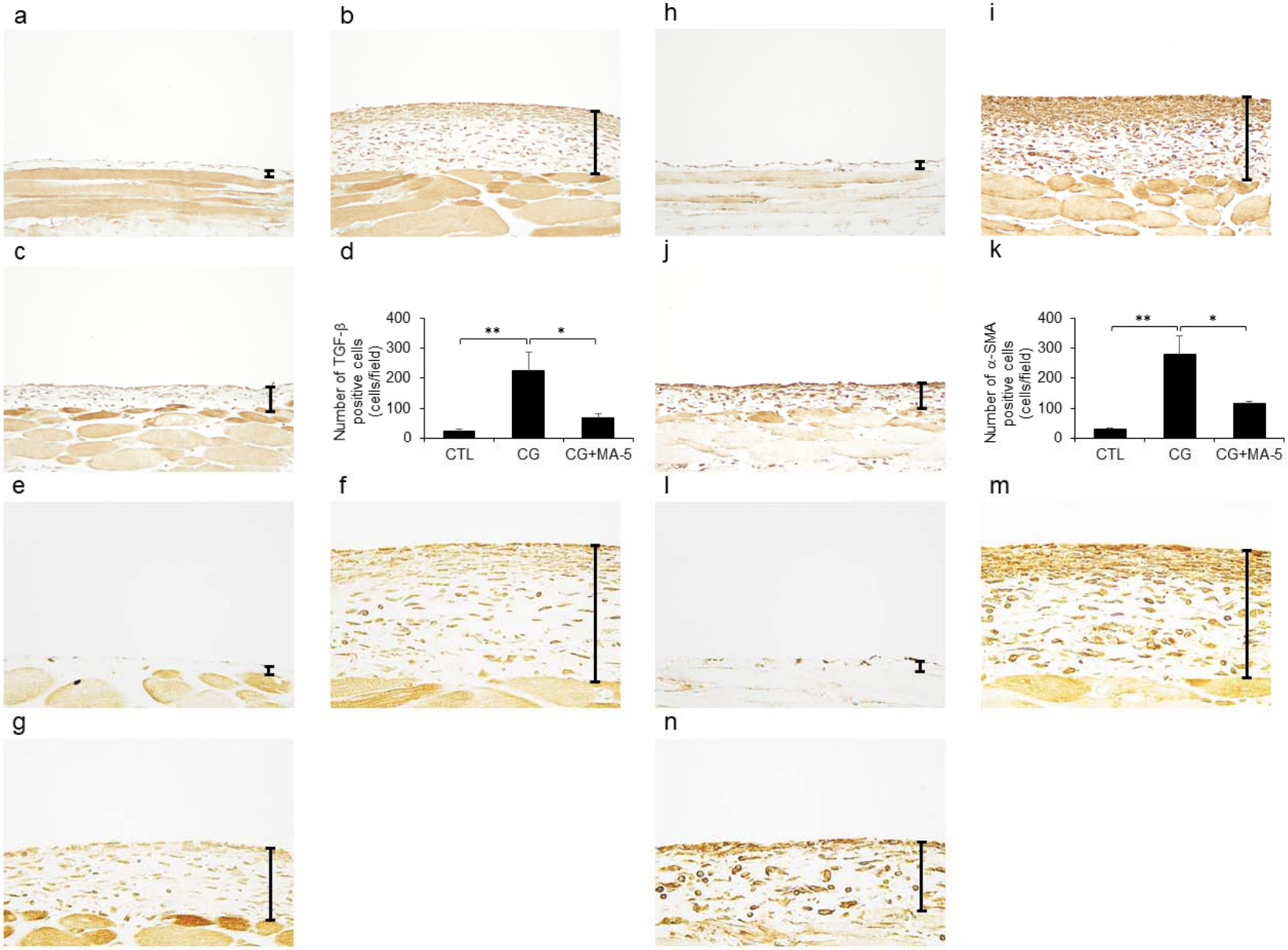
a
b
h
i
c
d
j
k
e
f
l
m
g
n
Number of TGF-β positive cells (cells/field)
400
300
200
100
0
**
*
CTL
CG
CG+MA-5
Number of α-SMA positive cells (cells/field)
400
300
200
100
0
**
*
CTL
CG
CG+MA-5

Figure 3

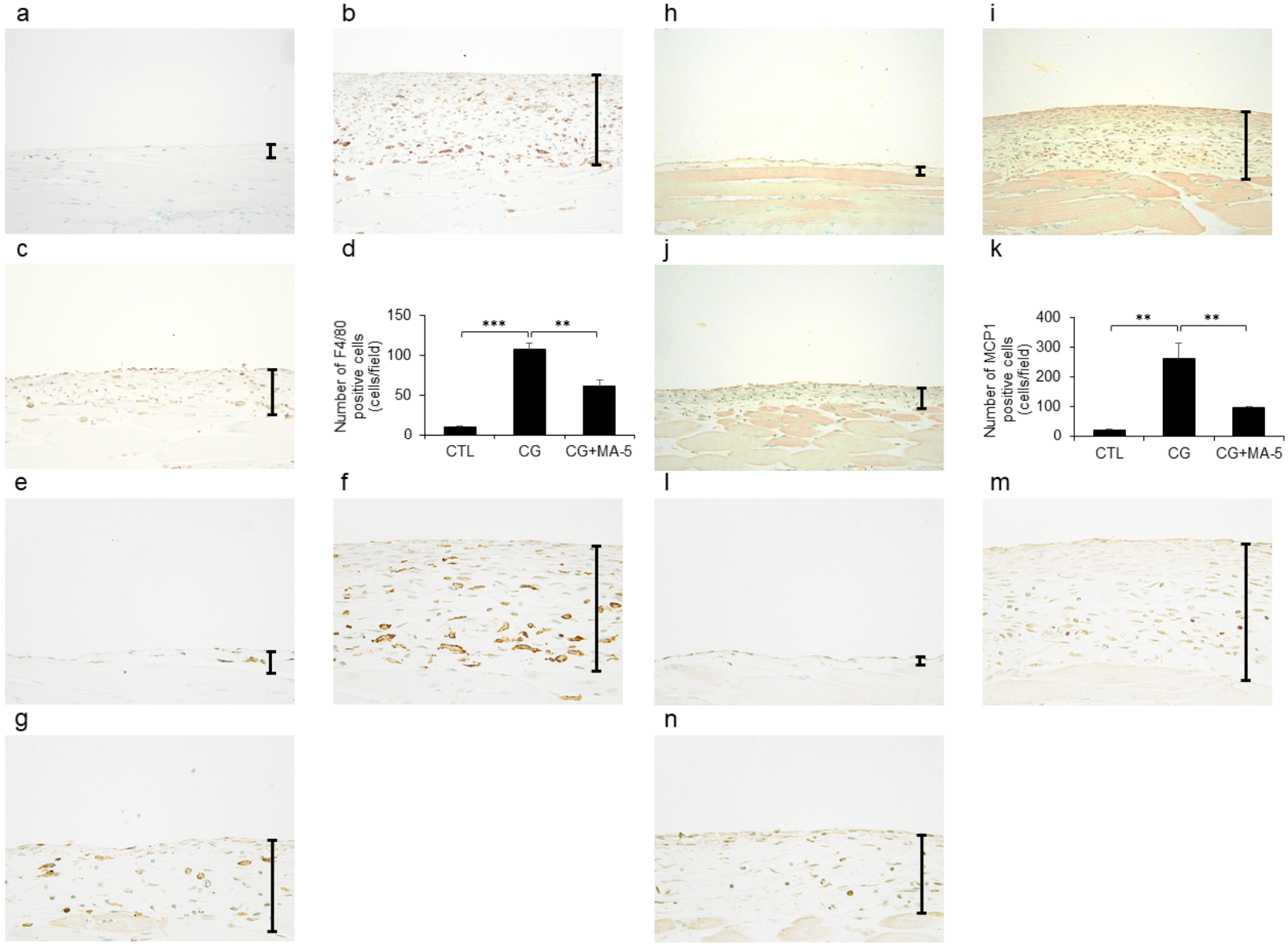
a
b
h
i
c
d
j
k
e
f
l
m
g
n
Number of F4/80 positive cells (cells/field)
150
100
50
0
***
**
CTL
CG
CG+MA-5
Number of MCP1 positive cells (cells/field)
400
300
200
100
0
**
**
CTL
CG
CG+MA-5

Figure 4

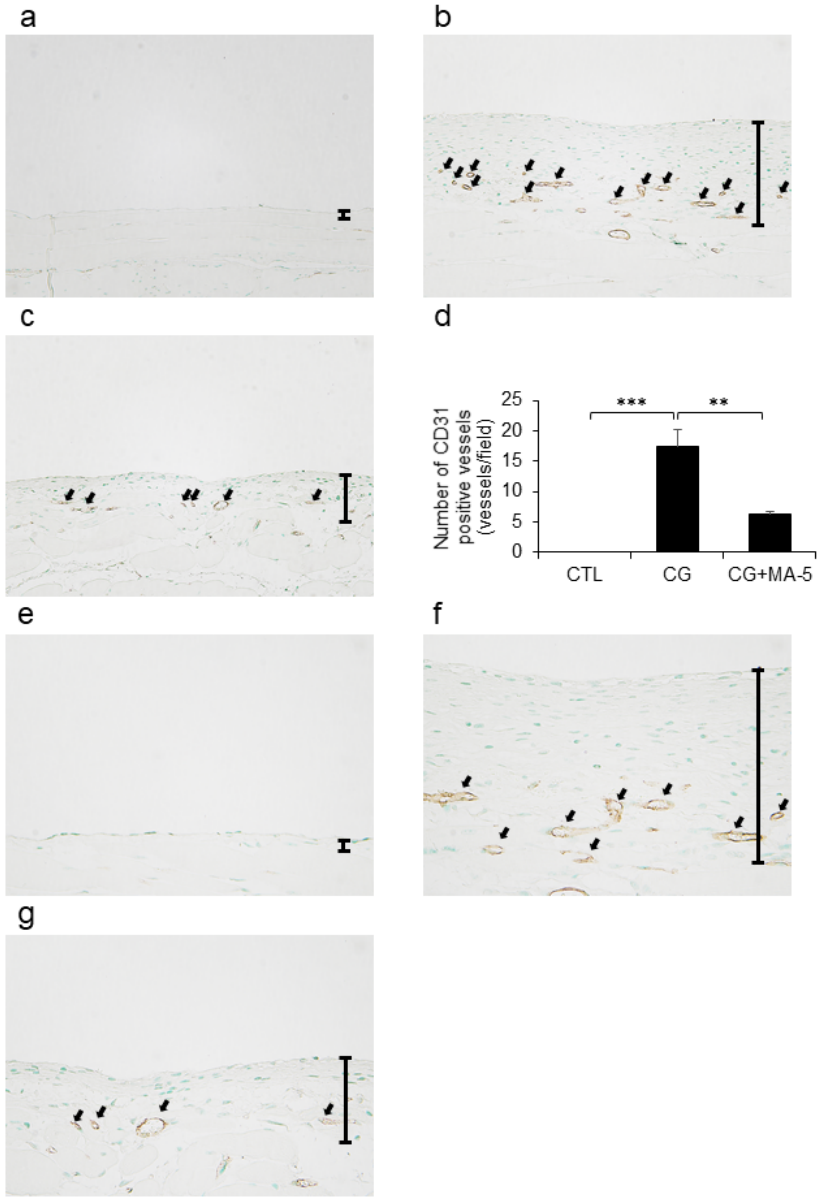
a
b
c
d
e
f
g
Number of CD31 positive vessels (vessels/field)
25
20
15
10
5
0
***
**
CTL
CG
CG+MA-5

Figure 5

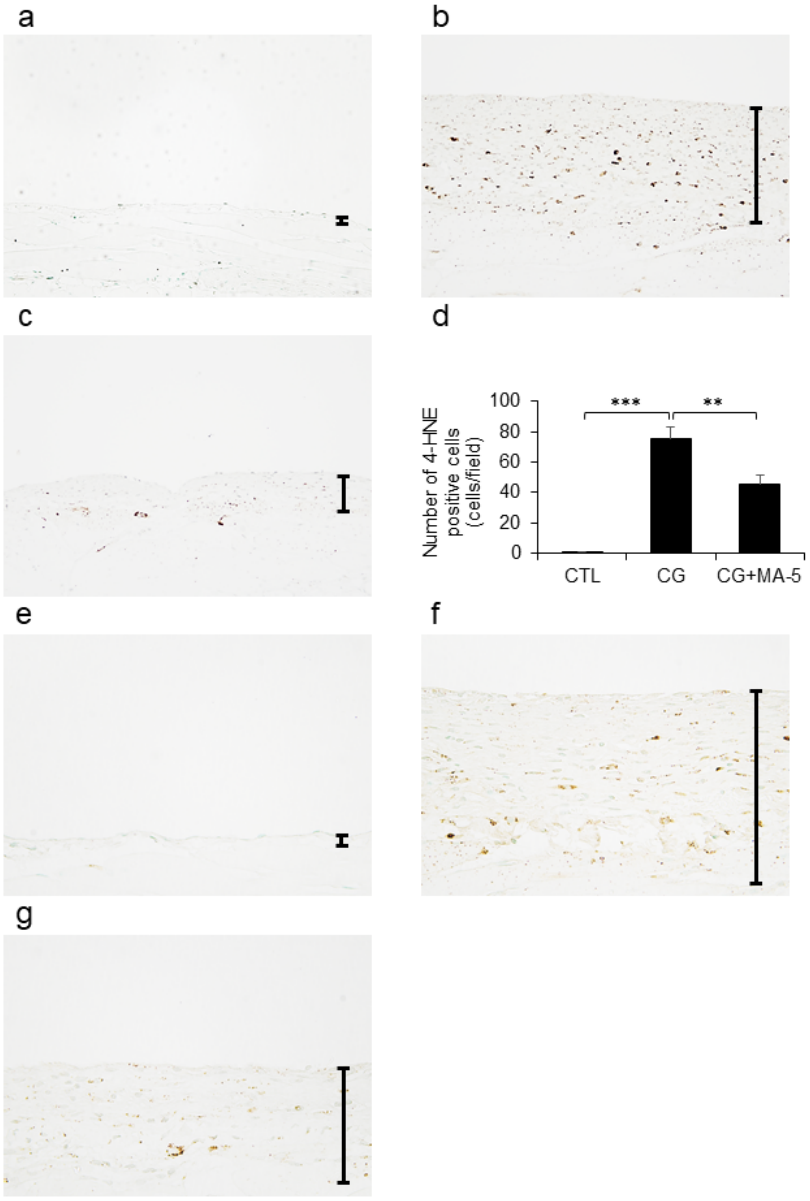
a
b
c
d
e
f
g
Number of 4-HNE positive cells (cells/field)
100
80
60
40
20
0
***
**
CTL
CG
CG+MA-5

Figure 6

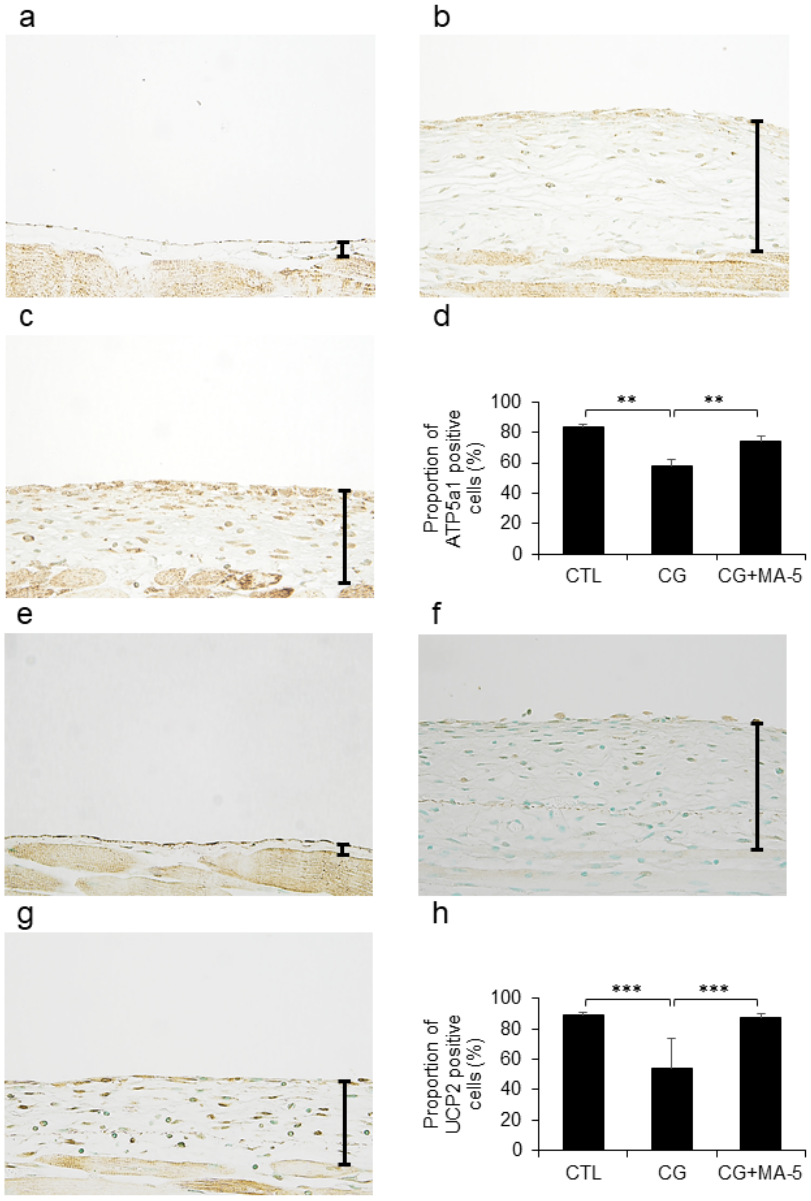
a
b
c
d
Proportion of ATP5a1 positive cells (%)
100
80
60
40
20
0
**
**
CTL
CG
CG+MA-5
e
f
g
h
Proportion of UCP2 positive cells (%)
100
80
60
40
20
0
***
***
CTL
CG
CG+MA-5

Figure 7

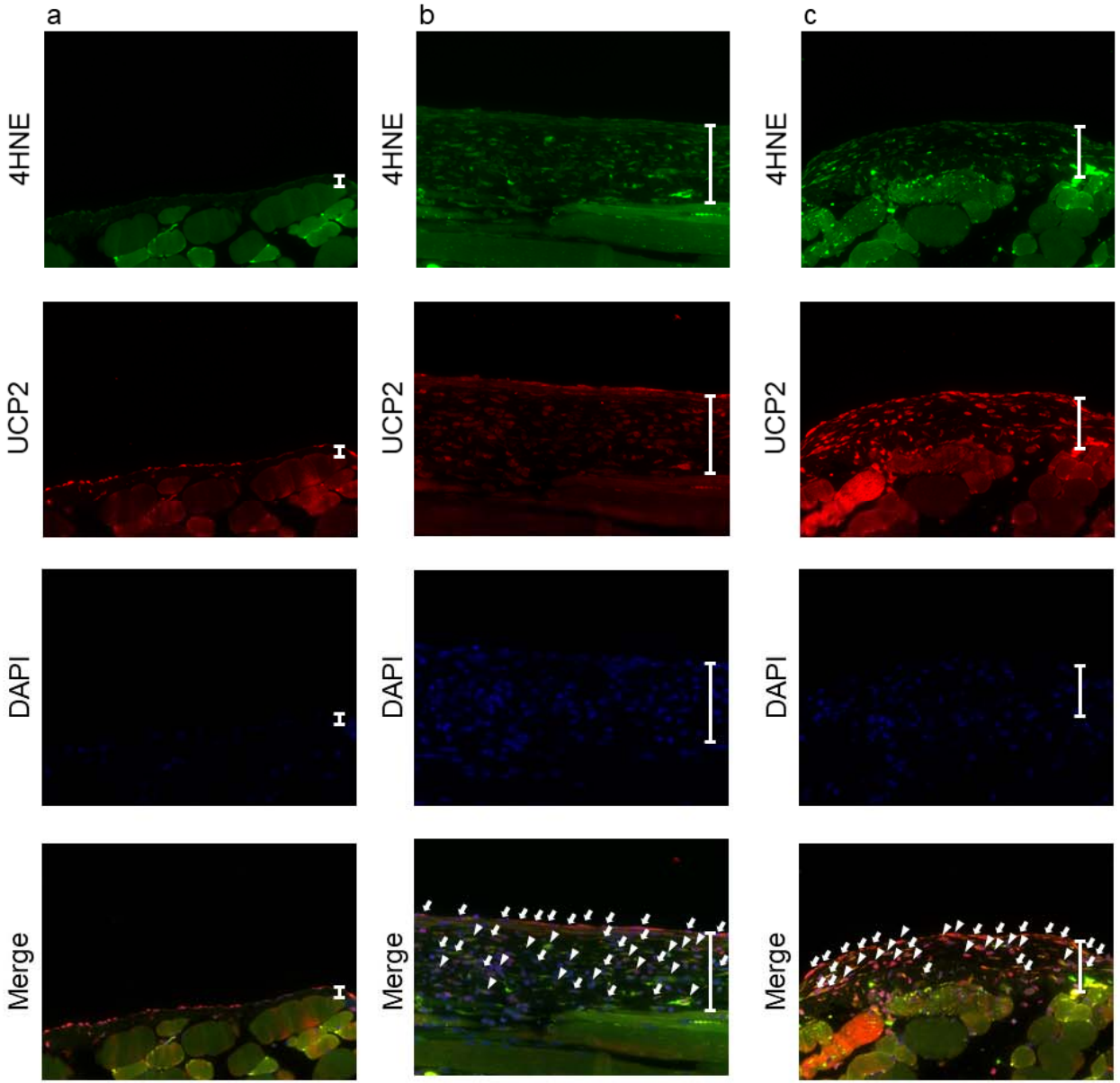

Online Resource 1

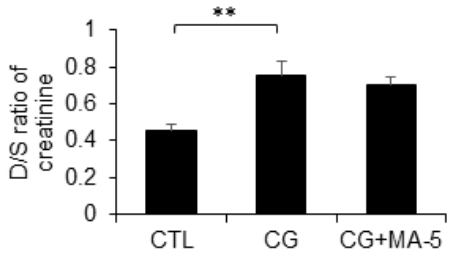

Online Resource 2

a

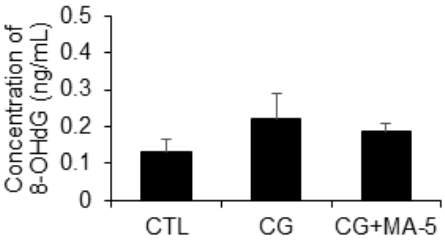

b

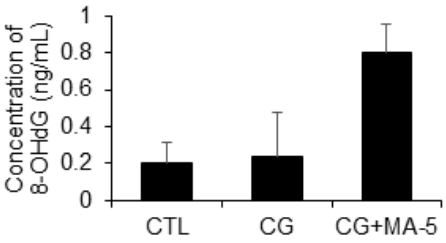

Online Resource 3